

PCCP

Accepted Manuscript



This is an *Accepted Manuscript*, which has been through the Royal Society of Chemistry peer review process and has been accepted for publication.

Accepted Manuscripts are published online shortly after acceptance, before technical editing, formatting and proof reading. Using this free service, authors can make their results available to the community, in citable form, before we publish the edited article. We will replace this *Accepted Manuscript* with the edited and formatted *Advance Article* as soon as it is available.

You can find more information about *Accepted Manuscripts* in the [Information for Authors](#).

Please note that technical editing may introduce minor changes to the text and/or graphics, which may alter content. The journal's standard [Terms & Conditions](#) and the [Ethical guidelines](#) still apply. In no event shall the Royal Society of Chemistry be held responsible for any errors or omissions in this *Accepted Manuscript* or any consequences arising from the use of any information it contains.

The UV Absorption Spectrum of the Simplest Criegee Intermediate CH₂OO

Wei-Lun Ting¹, Ying-Hsuan Chen¹, Wen Chao,^{1,2} Mica C. Smith,^{1,3} Jim Jr-Min Lin^{1,2,4*}

¹ Institute of Atomic and Molecular Sciences, Academia Sinica, Taipei 10617, Taiwan

² Department of Chemistry, National Taiwan University, Taipei 10617, Taiwan

³ Department of Chemistry, University of California at Berkeley, Berkeley, CA 94720, USA

⁴ Department of Applied Chemistry, National Chiao Tung University, Hsinchu 30010, Taiwan

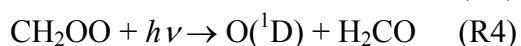
Abstract

SO₂ scavenging and self-reaction of CH₂OO were utilized for the decay of CH₂OO to extract the absorption spectrum of CH₂OO in bulk conditions. Absolute absorption cross sections of CH₂OO at 308.4 and 351.8 nm were obtained from laser-depletion measurements in a jet-cooled molecular beam. The peak cross section is $(1.23 \pm 0.18) \times 10^{-17} \text{ cm}^2$ at 340 nm.

*Email: jimlin@gate.sinica.edu.tw

† Electronic supplementary information (ESI) available.

Ozonolysis is a major removal mechanism in the troposphere for unsaturated hydrocarbons which are emitted in large quantities from both natural and human sources. Now it is generally accepted that ozonolysis of alkenes proceeds via Criegee intermediates, highly reactive species postulated in 1949 by Rudolf Criegee.^{1,2} In the troposphere, Criegee intermediates are involved in several important atmospheric reactions,³ including reactions with SO₂ and NO₂,^{4,5,6,7} or can be photolyzed by near UV light,^{7,8,9,10} as shown for CH₂OO in (R1)–(R4).

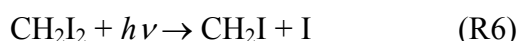


The formation of SO₃ and NO₃, as in (R2) and (R3), plays an important role in atmospheric chemistry,^{11,12} including aerosol and cloud formation. The formation of O(¹D), as in (R4), will result in OH formation through (R5).



Because CH₂OO absorbs strongly at wavelengths longer than 300 nm,^{7–9} tropospheric photolysis of CH₂OO would be quite efficient with an effective photolysis lifetime on the order of 1 second.⁸ As a result, the OH formation of (R4)+(R5) may contribute significantly to the atmospheric OH concentrations.

Despite their importance, the direct detection of Criegee intermediates was not realized until recently.^{4,13} Welz et al.⁴ reported an efficient way to prepare Criegee intermediates. For example, CH₂OO can be prepared via (R6)+(R7a).



Welz et al.⁴ also demonstrated the direct detection of CH₂OO by using vacuum UV photoionization mass spectrometry. The parent ion CH₂O₂⁺ was observed when the photon energy exceeded the ionization energy of CH₂OO (10.0 eV).⁴ Other isomers like dioxirane and formic acid are excluded due to their different ionization energies. At low pressure, the yield of (R7a) is close to unity,^{14,15} while the adduct formation (R7b) may dominate at near atmospheric pressures.¹⁴



The kinetics of CH₂OO reactions with SO₂ and NO₂ were investigated by Welz et al.⁴ and by Stone et al.⁵ by observing the disappearance of CH₂OO and by detecting the H₂CO products, respectively. The rate coefficients of these reactions were found to be unexpectedly rapid and imply a substantially greater role of Criegee intermediates in models of tropospheric sulfate and nitrate chemistry.

Beames et al.⁸ recorded the UV spectrum of CH₂OO through observing its depletion in a molecular beam upon laser irradiation (an action spectrum). Based on their laser pulse energy and spot size, Beames et al.⁸ roughly estimated the peak absorption cross section to be $5 \times 10^{-17} \text{ cm}^2$ (at 335 nm with FWHM ~ 40 nm). Lehman et al.¹⁰ measured the angular and velocity distributions of O(¹D) photoproduct arising from UV excitation of CH₂OO in the 300–365 nm range. From the observed anisotropic angular distribution ($\beta \cong 0.97$), the authors concluded that the orientation of the transition dipole moment reflects the $\pi^* \leftarrow \pi$ character of the electronic transition associated with the COO group. The significant anisotropy of the photofragments also indicates the dissociation is faster than rotation.

Su et al.¹⁶ reported an infrared (IR) absorption spectrum of CH₂OO. By comparing their experimental results with high-level ab initio calculations, the authors concluded that the observed vibrational frequencies are more consistent with a zwitterion structure rather than a diradical structure. With IR detection, the same group¹⁷ found the self-reaction of CH₂OO is extremely fast, with a rate coefficient of $(4 \pm 2) \times 10^{-10} \text{ cm}^3 \text{ s}^{-1}$, which reflects a unique property of the zwitterionic character.

Sheps⁷ used a cavity-enhanced technique to measure UV absorption spectrum of CH₂OO and observed significant vibrational structures at the long wavelength side of the absorption band. Moreover, the absorption spectrum⁷ differs significantly from the action spectrum reported by Beames et al.⁸ Sheps' argument⁷ is the following. *“The difference between the absorption and action spectra likely arises from excitation to long-lived \tilde{B} (¹A') vibrational states that relax to lower electronic states by fluorescence or nonradiative processes, rather than by photodissociation.”* However, the measurement of the photoproduct anisotropy¹⁰ indicates the photodissociation is faster than rotation which is in the picosecond time scale. Thus, the slower fluorescence process cannot compete with the fast dissociation. Furthermore, there is no theoretical evidence for the nonradiative processes. To investigate the source of this difference, we re-investigate the UV spectrum of CH₂OO with two new methods.

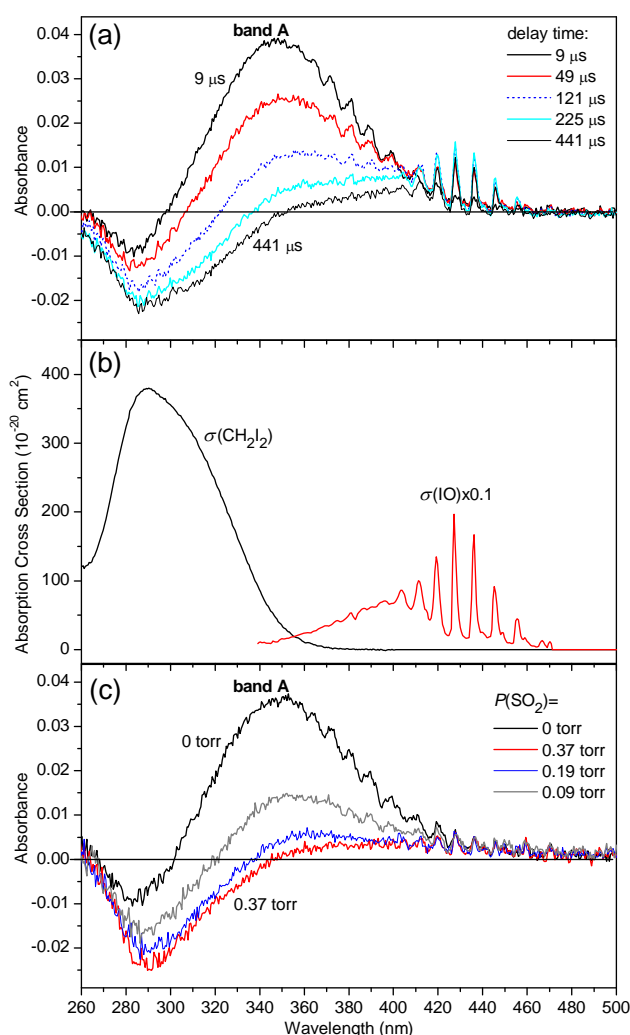


Figure 1. (a) Examples of the transient absorption spectra. The $[\text{CH}_2\text{I}_2]_0$, $[\text{O}_2]_0$ and the total number density n_{total} (N_2 balance) are 1.6×10^{15} , 3.4×10^{17} and $2.0 \times 10^{18} \text{ cm}^{-3}$, respectively. The depletion of CH_2I_2 ($< 10\%$ of $[\text{CH}_2\text{I}_2]_0$) results in negative absorbance peaked at $\sim 290 \text{ nm}$. The broad and strong absorption band peaked at $\sim 340 \text{ nm}$ (band A) is most likely due to CH_2OO , which is short-lived. At longer delay times, the formation of IO gives sharp peaks in the 410–460 nm range. (b) Published spectra of CH_2I_2 and IO.¹⁸ (c) Examples of transient absorption spectra at different SO_2 concentrations. It is clear that the intensity of band A decreases at higher SO_2 concentrations. $[\text{CH}_2\text{I}_2]_0$, $[\text{O}_2]_0$, and n_{total} are 1.3×10^{15} , 1.6×10^{18} , $3.3 \times 10^{18} \text{ cm}^{-3}$, respectively; delay time = 10.6 μs .

CH_2OO was prepared in a pulse-photolysis cell following the well-established method of $\text{CH}_2\text{I}_2/\text{O}_2$ photolysis.^{4,16} CH_2I_2 mixed with O_2 and N_2 was photolyzed at 248 nm (KrF excimer laser); transient absorption spectra were recorded by a gated intensified CCD camera (1 μs gate width) after the probe light was dispersed by a grating monochromator.^{19,20} See ESI for the experimental details. Figure 1a shows examples of the transient absorption spectra. In Figure 1a the most significant feature is a strong and broad absorption band peaked at $\sim 340 \text{ nm}$ which showed up quickly upon

photolysis and decayed with time. In addition, depletion of the CH_2I_2 precursor near 290 nm and formation of IO with distinct peaks near 430 nm were clearly observed, especially at long delay times.

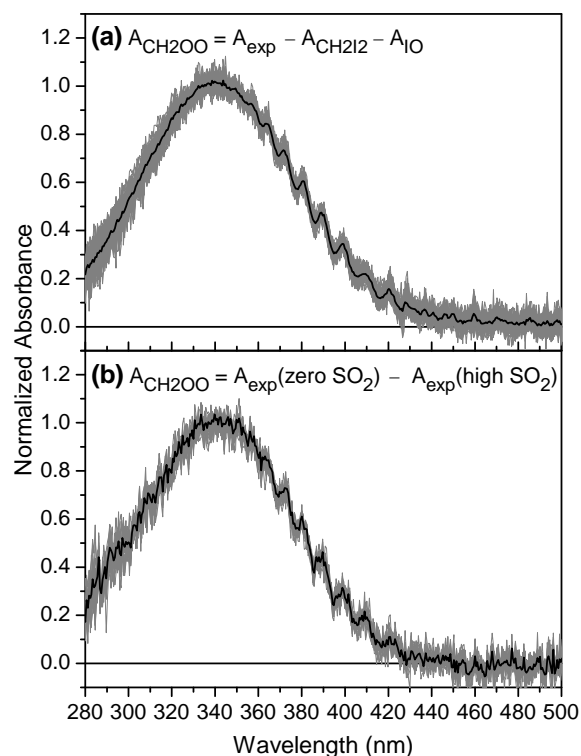


Figure 2. (a) Background-corrected height-normalized spectra of CH_2OO . The variation of the experimental parameters includes combinations of delay time (2–50 μs) and gas composition (O_2 percentage: 17–99%, N_2 balance), total pressure (7.5–100 torr), laser fluence (8–16 mJ/cm^2), etc. A total of 99 spectra (gray lines) and their average (black line) are plotted. (b) Height-normalized spectra of CH_2OO obtained by subtracting the experimental spectra at different SO_2 concentrations. A total of 24 spectra (gray lines) and their average (black line) are plotted. Delay time: 6.5–50 μs ; $[\text{SO}_2]$: $2.9 \times 10^{15} - 1.2 \times 10^{16} \text{ cm}^{-3}$.

Under our experimental conditions, CH_2OO reacted quickly with itself¹⁷ and with I atoms to form H_2CO , O_2 , and IO. Because H_2CO and O_2 absorb rather weakly, the transient spectra at long delay times mainly consist of the absorption changes of CH_2I_2 (depletion) and IO (formation). Since the spectra of CH_2I_2 and IO are very different, their contributions to the transient absorption spectra can be extracted and removed (see ESI for details). The remaining spectra are shown in Figure 2a. Consistent with Ref. 14, we did not observe significant difference in the CH_2OO yield upon O_2 mixing ratio. The identical shape of these spectra under various experimental conditions (delay times, laser fluences, and O_2 pressures) strongly suggests that the spectral carrier is a single species. Based on the high yield of CH_2OO from the $\text{CH}_2\text{I}_2/\text{O}_2$ photolysis at low pressure,^{14,15} it is most reasonable to assign the spectral carrier to CH_2OO (see below for discussion on the pressure dependence). If another absorbing species contributes significantly to these spectra, this species must exhibit kinetic

behavior similar to that of CH₂OO.

It is known that CH₂OO reacts quickly with SO₂ ($k_2 \sim (3-4) \times 10^{-11} \text{ cm}^3/\text{s}$).^{4,5} We utilized this kinetic signature of CH₂OO to examine the spectral carrier of band A. As shown in Figure 1c, it is clear that the intensity of band A decreases at higher SO₂ concentrations. Because the absorption cross sections of SO₂, H₂CO and SO₃ in the 316–450 nm range are much smaller ($< 1 \times 10^{-19} \text{ cm}^2$) than those of CH₂OO (peak cross section $> 1 \times 10^{-17} \text{ cm}^2$),⁸ the differences between the spectra of Figure 1c should be mostly due to the absorption of CH₂OO. The height-normalized curves of such difference spectra are shown in Figure 2b. The nice agreement between Figures 2a and 2b confirms the above assignment.

When O₂ was absent in the photolysis cell, the absorption of CH₂I was present and band A could not be observed. With the published absorption cross sections of CH₂I,²¹ the initial number density of CH₂I can be estimated. Under the high O₂ pressures used, CH₂I reacted with O₂ within a few microseconds.^{5,7,14,15} Therefore the number density of CH₂OO can be estimated based on the published quantum yield of (R7a) ($\Phi_{\text{CH}_2\text{OO}} = 86\%$ at 11 torr).¹⁴ From the estimated number density and the observed absorbance of CH₂OO, its absolute peak cross section can be deduced to be $(1.26 \pm 0.25) \times 10^{-17} \text{ cm}^2$ at 340 nm. The overall error bar is estimated to be $\pm 20\%$ mostly due to the uncertainty in $\Phi_{\text{CH}_2\text{OO}}$.^{14,15} See ESI for details.

In Figure 2a we can see that the shape of band A does not depend on the total pressure in the range of 8–100 torr. This observation excludes the contribution of ICH₂OO because its formation is a termolecular process which has strong pressure dependence.^{14,15} At higher pressures (100 torr $< P <$ 760 torr), the yield of CH₂OO was found to decrease with pressure (see Table S1 for a typical example) and an additional (weaker) absorption band was observed at $\lambda < 290 \text{ nm}$, indicating formation of a new species (likely ICH₂OO).^{21,22} The absorption of ICH₂OO seems much weaker than that of CH₂OO, such that the change in spectral shape (not including the yield) with pressure is not very obvious.

The IO peaks are absent in short delay times while the absorption of CH₂OO is very significant, indicating IO is not a primary product. Based on our signal-to-noise ratio, we further constrain the primary IO yield to be less than 1%, resolving some debate among published results.^{23,24,25,26} The formation of IO is likely due to (R8).^{5,14}



Detailed kinetic analysis is beyond the scope of this paper and will be published elsewhere.

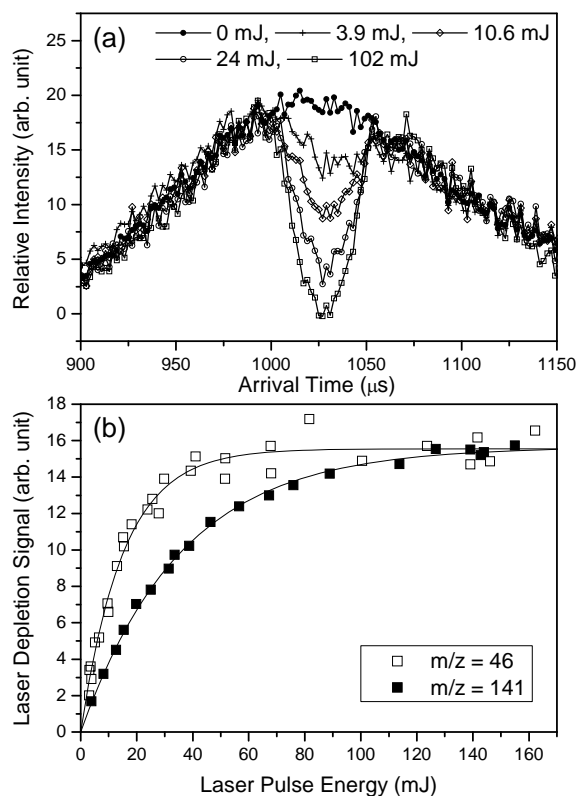


Figure 3. (a) Arrival-time profiles of CH_2OO at various laser fluences at 308.4 nm. The parent ion of CH_2OO was detected at $m/z = 46$ amu. (b) Saturation curve for the laser depletion of CH_2OO ($m/z=46$) and CH_2I_2 ($m/z=141$, CH_2I^+ , a daughter ion of CH_2I_2) at 308.4 nm. The x-axis is the laser pulse energy which is proportional to the laser fluence. The lines are the fit of eqn (1). The nice fit indicates the laser depletion experiments are single-photon processes.

To further quantify the absolute value of the absorption cross section of CH_2OO , we measured the depletion of CH_2OO in a molecular beam upon laser irradiation at 308.4 and 351.8 nm. CH_2OO was detected with a quadrupole mass spectrometer equipped with an electron impact ionizer. This method^{27,28,29} has been demonstrated to be efficient in determining the photodissociation cross section of a species in a mixture without knowledge of its concentration. Under our experimental conditions, the number of molecules N after laser irradiation can be described by eqn (1).

$$\frac{N}{N_0} = e^{-I\sigma\phi} \quad \frac{\Delta N}{N_0} = 1 - e^{-I\sigma\phi} \quad (1)$$

Where N_0 is the number of molecules before the laser irradiation, I is the laser fluence in photons per cm^2 , σ is the absorption cross section in cm^2 , ϕ is the dissociation quantum yield and $\Delta N = N_0 - N$. For CH_2I_2 , the excitations at 351.8 and 308.4 nm correspond to repulsive (unbound) excited states which dissociate in picosecond time scales,^{30,31,32} resulting in 100% dissociation ($\phi = 1$).

Figure 3a shows the arrival-time profiles of CH_2OO at various laser fluences at 308.4 nm. Figure 3b

is the corresponding saturation curve. A nice fit of eqn (1) to the experimental data indicates the measurement corresponds to a single species (or multiple species having the same cross section, which is unlikely). The results at 351.8 nm are similar (see ESI). The complete depletion of CH₂OO indicates its dissociation yield is unity. The absolute cross section of CH₂OO can be obtained by comparing its saturation curve with that of CH₂I₂, for which the cross section is known. A summary of the cross section measurement is shown in Table 1.

Table 1. Summary of the cross section measurements of CH₂OO in a jet-cooled molecular beam.

Wavelength (nm)	$\frac{\sigma\phi(\text{CH}_2\text{OO})}{\sigma\phi(\text{CH}_2\text{I}_2)}$	$\sigma(\text{CH}_2\text{I}_2)$ (cm ²) ^b	$\sigma(\text{CH}_2\text{OO})$ (cm ²)
308.4	2.52±0.28 ^a	3.21×10 ⁻¹⁸	(8.09±0.90)×10 ⁻¹⁸
351.8	47.6±5.2	≤ 2.54×10 ⁻¹⁹	≤ (1.21±0.13)×10 ⁻¹⁷

^a The error bar is 2 standard deviation.

^b Average values of Refs. 33 and 34 at $T = 273$ K. The temperature dependence of the UV absorption cross section of CH₂I₂ is very weak at 308.4 nm, but moderate at 351.8 nm.³⁴ The actual cross section at 351.8 nm would be smaller for CH₂I₂ in a jet-cooled molecular beam.

With the absolute cross sections of CH₂OO (Table 1), we may set the spectra of Figure 2 on the absolute scale. However, we need to consider the temperature effect of the absorption cross sections because the temperature of the molecular beam is lower than room temperature. Since the cross section of CH₂I₂ at 308.4 nm does not change with temperature,^{33,34} we can use the near-room-temperature value for the cross section of CH₂I₂ in a molecular beam. The UV absorption band of CH₂OO can be assigned to the intense $\tilde{\text{B}} \leftarrow \tilde{\text{X}}$ transition^{8,22} which is analogous to the Hartley band of O₃. The cross section of the O₃ Hartley band has a quite weak temperature dependence.^{18,35} The peak cross section (at 254 nm) of O₃ increases by ~1.5% when the temperature decreases from 293 K to 203 K. For the main region of the Hartley band (215–288 nm, $1 \times 10^{-18} \text{ cm}^2 < \sigma < 1.1 \times 10^{-17} \text{ cm}^2$), the temperature effect is within 5% (203–293 K).^{18,35} Similarly, it is expected that the temperature dependence of the CH₂OO cross sections is weak near the peak. Therefore, we choose the cross section at 308.4 nm to scale the average spectra of Figure 2 and to plot the scaled spectra in Figure 4. We believe the SO₂ scavenging method would give a more reliable spectrum of CH₂OO (see Table S3 for numerical values) while the result of the self-reaction method is very similar. The peak value of the scaled spectrum is (1.23±0.18)×10⁻¹⁷ cm² at 340 nm. We assume an error bar of ±15% to include possible variations due to the temperature effect. This value is consistent with the peak cross section of (1.26±0.25)×10⁻¹⁷ cm² obtained in the transient absorption experiment of this work based on the estimated CH₂OO number density.

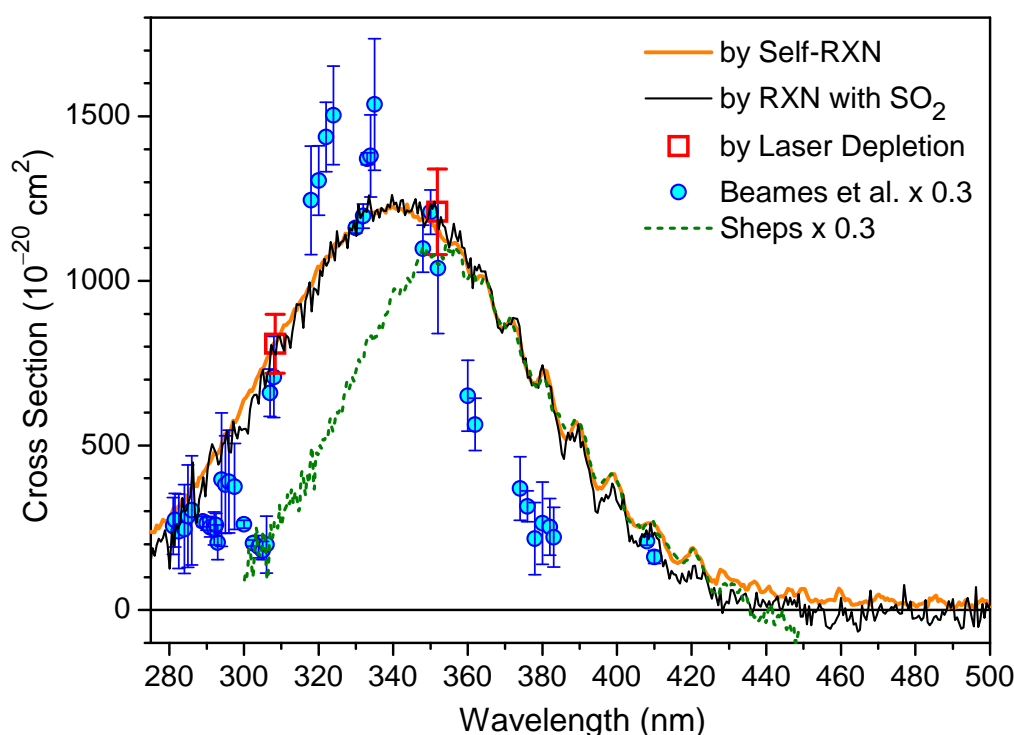


Figure 4. Absorption spectrum of CH_2OO . The thick orange and thin black lines are the average curves of Figure 2a and 2b, respectively. For the thin black line (numerical values can be found in ESI), the absorbance due to the reacted SO_2 has been removed, based on the mass balance of (R2) (See ESI). Square symbols are the absolute cross sections from the molecular beam-laser depletion measurements (Table 1). The black and orange lines are scaled to match the absolute cross section at 308.4 nm. The results of Sheps⁷ and Beames et al.⁸ are scaled by a factor of 0.3 for easier comparison. The temperature of the photolysis cell was 295 K. The molecular beams of this work and Beames et al.⁸ were jet-cooled (estimated rotational temperature ~ 10 K).

Previous UV absorption⁷ and action spectra⁸ of CH_2OO exhibit significant differences. Beames et al.⁸ measured the laser depletion of CH_2OO in a similar molecular beam and obtained an action spectrum of CH_2OO . However Beames et al.⁸ only estimated the laser fluence from their laser (a dye laser) pulse energy and spot size. The beam spot of a dye laser is usually highly non-uniform. Without using a laser beam profiler, it is difficult to quantify the actual laser fluence. Beames et al.⁸ might underestimate their laser fluence and thus overestimate the CH_2OO cross section. In this work, we utilized a reference molecule to effectively calibrate the laser fluence and to cancel the effect of non-uniform laser spot.³⁶ Therefore, our results should be more accurate.

Figure 4 compares our results with those of Sheps⁷ and Beames et al.⁸ The scaled spectrum of Beames et al.⁸ is weaker at $\lambda \geq 360$ nm. The temperature effect may be one possible reason for this difference. While the intense Hartley band of O_3 has a rather weak temperature dependence, the

weak Huggins band or the long-wavelength tail of the Hartley band (310–380 nm) has very strong temperature dependence (smaller cross sections at lower temperatures).^{18,35} If the temperature dependence of the CH₂OO cross sections at $\lambda \geq 360$ nm is as strong as that of the Huggins band of O₃, this may explain why the spectrum of Beames et al.⁸ is weaker in this wavelength range. Another possibility mentioned by Sheps⁷ is a decrease in the dissociation yield at long wavelengths. Although this might explain the discrepancy between the absorption and action spectra, it is inconsistent with the product anisotropy measurement by Lehman et al.¹⁰ which shows that the UV photodissociation of CH₂OO is faster than its rotation (~ picosecond). Thus, a non-unity dissociation yield would require a fast process that can compete with photodissociation. Fluorescence is too slow to fulfill this condition. Other fast non-radiative processes are unlikely but cannot be fully ruled out at this moment. More evidence and investigations are needed.

Sheps⁷ used a newly-built cavity-enhanced absorption spectrometer to measure the transient absorption spectra of CH₂I₂/O₂ photolysis system. Sheps⁷ determined the absolute CH₂OO spectrum based on the measured CH₂I spectrum (when O₂ was absent) and an estimated (90±10)% yield of transforming CH₂I to CH₂OO at 5 torr. Qualitatively, the shape of Sheps' spectrum⁷ is similar to ours, particularly the structures at the long-wavelength side (the peak positions are matched). However, the short-wavelength side of Sheps' spectrum⁷ decays much faster than that of this work. Furthermore, the reported peak cross section and position of the CH₂OO spectrum by Sheps⁷ [(3.6±0.9)×10⁻¹⁷ cm² at 355 nm] are different from our values. The source of the discrepancies is not clear. It might arise from the complexity of the cavity-enhanced measurement.

There are at least 7 vibrational peaks observable on the long-wavelength side of the UV absorption band of CH₂OO (Figures 2 and 4). The widths of these vibrational peaks are significantly wider than the instrument resolution of ~2 nm. Similar structures have been reported by Sheps⁷ at slightly lower resolution and signal-to-noise ratio. The positions of the most well-defined peaks are 363.7, 372.0, 380.7, 389.2, 399.0, 409.3, 420.5 nm (27495, 26882, 26267, 25694, 25063, 24432, 23781 cm⁻¹). The average peak separation is about 620 cm⁻¹. Analogous to the Huggins band of O₃, these vibrational structures may arise from some periodic motions on the excited potential energy surface, most likely the $\tilde{B}(^1A')$ surface. The widths of the vibrational peaks may originate from congested vibrational structures (vibrational modes involving O–O stretching and C–O–O bending)²² or rotational contours at room temperature. For the O₃ Huggins band, the widths of the vibrational peaks become narrower at low temperatures.^{18,35} It will be interesting to see how the peak structures change at lower temperatures for CH₂OO.

In summary, more accurate UV absorption cross sections of the simplest Criegee intermediate CH₂OO are reported. The peak cross section is determined to be (1.23±0.18)×10⁻¹⁷ cm² at 340 nm. This value is significantly smaller than previous reports,^{7,8} implying slower photolysis rates in the

atmosphere than previously expected. Nonetheless, this intense absorption band of CH₂OO overlaps well with the incoming solar spectrum, resulting in efficient photolysis for this Criegee intermediate. The clear vibrational structures on the long-wavelength side of the CH₂OO spectrum provide a fingerprint feature for spectroscopic identification of this elusive intermediate.

Acknowledgements: This work was supported by Academia Sinica and Ministry of Science and Technology, Taiwan (NSC100-2113-M-001-008-MY3). The authors thank Miss Shu-Yi Meng for assistance in data acquisition and Profs. Yuan T. Lee and Yuan-Pern Lee for discussions.

References:

- 1 R. Criegee, *Angew. Chem., Int. Ed.*, 1975, 14, 745–752.
- 2 R. Criegee and G. Wenner, *Liebigs Ann. Chem.*, 1949, 564, 9–15.
- 3 C. A. Taatjes, D. E. Shallcross and C. Percival, *Phys. Chem. Chem. Phys.*, 2014, 16, 1704–1718. DOI: 10.1039/C3CP52842A.
- 4 O. Welz, J. D. Savee, D. L. Osborn, S. S. Vasu, C. J. Percival, D. E. Shallcross and C. A. Taatjes, *Science*, 2012, 335, 204–207.
- 5 D. Stone, M. Blitz, L. Daubney, N. U. M. Howesa and P. Seakins, *Phys. Chem. Chem. Phys.*, 2014, 16, 1139–1149. DOI: 10.1039/c3cp54391a.
- 6 Bin Ouyang, Matthew W. McLeod, Roderic L. Jones and William J. Bloss, *Phys. Chem. Chem. Phys.*, 2013, 15, 17070–17075
- 7 L. Sheps, *J. Phys. Chem. Lett.* 2013, 4, 4201–4205.
- 8 J. M. Beames, F. Liu, L. Lu and M. I. Lester, *J. Am. Chem. Soc.*, 2012, 134, 20045–20048.
- 9 J. M. Beames, F. Liu, L. Lu and M. I. Lester, *J. Chem. Phys.*, 2013, 138, 244307.
- 10 J. H. Lehman, H. Li, J. M. Beames and M. I. Lester, *J. Chem. Phys.*, 2013, 139, 141103.
- 11 Carl J. Percival et al., *Faraday Discuss.*, 2013, 165, 45–73.
- 12 M. Boy, D. Mogensen, S. Smolander, L. Zhou, T. Nieminen, P. Paasonen, C. Plass-Dülmer, M. Sipilä, T. Petäjä, L. Mauldin, H. Berresheim, and M. Kulmala, *Atmos. Chem. Phys.*, 2013, 13, 3865–3879.
- 13 C. A. Taatjes, G. Meloni, T. M. Selby, A. J. Trevitt, D. L. Osborn, C. J. Percival and D. E. Shallcross, *J. Am. Chem. Soc.*, 2008, 130, 11883–11885.
- 14 D. Stone, M. Blitz, L. Daubney, T. Ingham and P. Seakins, *Phys. Chem. Chem. Phys.*, 2013, 15, 19119–19124.
- 15 H. Huang, A. J. Eskola and C. A. Taatjes, *J. Phys. Chem. Lett.*, 2012, 3, 3399–3403; H. Huang, B. Rotavera, A. J. Eskola and C. A. Taatjes, *J. Phys. Chem. Lett.*, 2013, 4, 3824.
- 16 Y.-T. Su, Y.-H. Huang, H. A. Witek and Y.-P. Lee, *Science*, 2013, 340, 174–176.

-
- 17 Y.-T. Su, H.-Y. Lin, R. Putikam, H. Matsui, M. C. Lin and Y.-P. Lee, *Nature Chemistry*, 2014, DOI:10.1038/nchem.1890.
- 18 S.P. Sander, J. Abbatt, J. R. Barker, J. B. Burkholder, R. R. Friedl, D. M. Golden, R. E. Huie, C. E. Kolb, M. J. Kurylo, G. K. Moortgat, V. L. Orkin and P. H. Wine "Chemical Kinetics and Photochemical Data for Use in Atmospheric Studies, Evaluation Number 17", JPL Publication 10-6, Jet Propulsion Laboratory, Pasadena, 2011. <http://jpldataeval.jpl.nasa.gov>
- 19 M.-N. Su and J. J. Lin, *Rev. Sci. Instrum.* 2013, 84 , 086106.
- 20 M.-N. Su and J. J. Lin, *GSTF Journal of Chemical Sciences (JChem)* (ISSN: 2339-5060) 2013, 1, 52–57. (DOI: 10.5176/2339-5060_1.1.6)
- 21 J. Sehested, T. Ellermann, and O.J. Nielsen, *Int. J. Chem. Kinet.*, 1994, 26, 259-272.
- 22 E. P. F. Lee, D. K. W. Mok, D. E. Shallcross, C. J. Percival, D. L. Osborn, C. A. Taatjes and J. M. Dyke, *Chem.–Eur. J.*, 2012, 18, 12411–12423.
- 23 T. J. Gravestock, M. A. Blitz, W. J. Bloss, D. E. Heard, *ChemPhysChem*, 2010, 11, 3928.
- 24 T. J. Dillon, M. E. Tucceri, R. Sander, J. N. Crowley, *Phys. Chem. Chem. Phys.*, 2008, 10, 1540.
- 25 A. J. Eskola, D. Wojcik-Pastuszka, E. Ratajczak and R. S. Timonen, *Phys. Chem. Chem. Phys.*, 2006, 8, 1416-1424.
- 26 S. Enami, T. Yamanaka, S. Hashimoto, M. Kawasaki, K. Tonokura and H. Tachikawa, *Chem. Phys. Lett.*, 2007, 445, 152–156.
- 27 H.-Y. Chen, C.-Y. Lien, W.-Y. Lin, Y. T. Lee, and J. J. Lin, *Science*, 2009, 324, 781.
- 28 Jim J. Lin, Andrew F Chen, and Yuan T. Lee, *Chem. Asian J.*, 2011, 6, 1664.
- 29 Bing Jin, Man-Nung Su, and Jim J. Lin, *J. Phys. Chem. A*, 2012, 116, 12082-12088 .
- 30 Jinzhong Zhang, Eric J. Heller, Daniel Huber, Dan G. Imre and David Tannor, *J. Chem. Phys.*, 1988, 89, 3602.
- 31 H.F. Xu, Y. Guo, S.L. Liu, X.X. Ma, D.X. Dai, G.H. Sha, *J. Chem. Phys.*, 2002,117, 5722.
- 32 Julia H. Lehman, Hongwei Li, Marsha I. Lester, *Chem. Phys. Lett.*, 2013, 590, 16–21.
- 33 J.C. Mössinger, D.E. Shallcross, and R.A. Cox, *J. Chem. Soc. Faraday Trans.*, 1998, 94, 1391-1396.
- 34 C.M. Roehl, J.B. Burkholder, G.K. Moortgat, A.R. Ravishankara, and P.J. Crutzen, *J. Geophys. Res.*, 1997, 102, 12819-12829.
- 35 W. Chehade, B. G^{ur}, P. Spietz, V. Gorschelev, A. Serdyuchenko, J. P. Burrows, and M. Weber, *Atmos. Meas. Tech.*, 2013, 6, 1623–1632.
- 36 B. Jin, I-C. Chen, W.-T. Huang, C.-Y. Lien, N. Guchhait, and J. J. Lin, *J. Phys. Chem. A*, 2010, 114, 4791.